

Graphical Abstract

Generalizable Graph Neural Networks for Robust Power Grid Topology Control

Matthijs de Jong, Jan Viebahn, Yuliya Shapovalova

Highlights

Generalizable Graph Neural Networks for Robust Power Grid Topology Control

Matthijs de Jong, Jan Viebahn, Yuliya Shapovalova

- Heterogeneous over homogeneous graphs increase graph neural network expressiveness
- Heterogeneous graph neural networks are the highest-performing models
- Graph neural networks generalize better to out-of-distribution networks
- Machine learning agents obtain good performance at high efficiency

Generalizable Graph Neural Networks for Robust Power Grid Topology Control

Matthijs de Jong^{a,b}, Jan Viebahn^{b,*}, Yuliya Shapovalova^a

^a*Radboud University, Houtlaan 4, Nijmegen, 6525 XZ, The Netherlands*

^b*TenneT TSO, Utrechtseweg 310, Arnhem, 6812 AR, The Netherlands*

Abstract

The energy transition necessitates new congestion management methods. One such method is controlling the grid topology with machine learning (ML). This approach has gained popularity following the Learning to Run a Power Network (L2RPN) competitions. Graph neural networks (GNNs) are a class of ML models that reflect graph structure in their computation, which makes them suitable for power grid modeling. Various GNN approaches for topology control have thus been proposed. We propose the first GNN model for grid topology control that uses only GNN layers. Additionally, we identify the busbar information asymmetry problem that the popular homogeneous graph representation suffers from, and propose a heterogeneous graph representation to resolve it. We train both homogeneous and heterogeneous GNNs and fully connected neural networks (FCNN) baselines on an imitation learning task. We evaluate the models according to their classification accuracy and grid operation ability. We find that the heterogeneous GNNs perform best on in-distribution networks, followed by the FCNNs, and lastly, the homogeneous GNNs. We also find that both GNN types generalize better to out-of-distribution networks than FCNNs.

Keywords: Power Grid Operation, Graph Neural Networks, Topology Control, Heterogeneous Graph Representation, Busbar Information Asymmetry, L2RPN, Out-of-Distribution Generalization

*Corresponding Author: Jan.Viebahn@tennet.eu; Utrechtseweg 310, Arnhem, 6812 AR, The Netherlands; +31 6 15 01 43 90

1. Introduction

The energy transition is crucial for ensuring society’s sustainability and future security. Transmission system operators (TSOs) play a crucial role in this transition. They are consequently facing new operational challenges [9]. Grid congestion is a problem that TSOs are already encountering but which the energy transition will exacerbate [42]. If not mitigated, grid congestion could make the future availability of energy unreliable.

There are several actions that TSOs can take to alleviate grid congestion [17]. Presently, redispatching and curtailment are the primary methods. However, these actions are often costly, disruptive, or not applicable. Topology control presents an opportunity for remedying grid congestion without these problems [41]. Congestion can be relieved by exploiting the flexibility in the network topology. However, this technique mostly remained unutilized, as the space of potential topologies is combinatorially large.

Due to the recent congestion management challenges, there has been a new interest in topology control. This interest led to the development of the GridOptions tool for remedial action recommendation by Viebahn et al. [41]. This tool validates the practical value of topology control. Even simple topological strategies could reduce line congestion by ten to twenty percent. The recommended strategies improved upon strategies without topological actions or those considered by grid operators. However, while the results are promising, further developments are necessary for broader applicability. The tool was only applied to a small subset of the Dutch power grid, featuring nine substations. Additionally, the inference time of the tool is relatively long: one hour. The next challenges involve scaling this approach and reducing inference time.

Machine learning (ML) presents a solution to these challenges [42]. ML models can learn which topologies are suitable in which situations and predict these topologies much quicker than traditional computational methods. To facilitate research in this area, the Learning to Run a Power Network (L2RPN) competitions were hosted [28, 27]. Furthermore, the Grid2Op Python library was developed.¹ This library greatly simplified the development and evaluation of ML methods for grid topology control. These developments kick-started research into ML methods for grid topology control.

¹<https://grid2op.readthedocs.io/>

Classical ML models are typically designed for tabular data and hence fail to capture the graph structure of power grids. This is problematic as the grid topology frequently changes, e.g., because of maintenance. Power grid operation requires adapting to such changes. Graph neural networks (GNNs) [36] are a class of ML models for graph-structured data. The computation in GNNs can reflect arbitrary graphs, which allows them to exploit a graph’s structure. This makes GNNs suitable for modeling power grids. GNNs have thus been applied to many grid operation tasks [5, 4, 31, 11, 18, 13, 30].

Various GNN approaches have been proposed for grid topology control [45, 43, 44, 35, 40, 33]. This research has demonstrated the feasibility of GNN approaches for grid topology control. However, important topics have not yet been addressed:

1. All approaches that directly predict topology actions with GNNs only use GNN layers as feature extractors or embedders [45, 43, 44, 33]. Fully-connected or attention layers follow the GNN layers. No research has investigated ‘fully graphical’ neural networks for grid topology control. Purely GNN approaches might be able to exploit the topology more deeply.
2. All present literature uses the graph representation specified by which busbars and power lines objects share. However, this is only one of many ways to represent the power grid as a graph. There has not been any study that compares graph representations and their effect on GNN performance.
3. Grid changes are frequent, and operation needs to continue despite these changes. For robust operation, models must generalize to potentially unexpected network states. A previous competition has focused on generalization to out-of-distribution injection profiles [27]. However, no work has investigated generalization to out-of-distribution networks.

This study aims to fill the aforementioned gaps in applying GNNs to grid topology control. We develop fully GNN models that use a richer graph representation. The main contributions of this study are:

1. We propose the first fully graphical neural network approach for grid topology control. The models are trained on a multi-label binary classification imitation learning task involving various networks and topologies. We compare the GNNs against fully connected neural networks (FCNNs). We evaluate the models by their classification accuracy and

ability to operate the power grid as agents. We also consider expert and hybrid agents and compare their inference speed.

2. We first analyze the effect of grid graph representation on GNN performance. The graph representation in the literature models current but not potential object-busbar attachments. This results in busbar information asymmetry, which blocks information flow and impairs GNN expressiveness. We propose a heterogeneous graph representation that models current and potential connections, which remedies busbar information asymmetry. We evaluate both graph representations with GNNs.
3. We first investigate the ability of graph neural networks to generalize topology control to out-of-distribution grids. Generalization is evaluated w.r.t. model accuracy and the ability of agents to operate the power grid, and contrasted against FCNNs.

This paper is organized as follows. Section 2 describes related work in ML grid topology control. Section 3 describes the power grid setup used in this study. Section 4 describes the methods used to develop the ML models. Section 5 describes the evaluation and analysis of the ML models. Sections 6 and 7 provide discussion and recommendations for future work, respectively. The code for this project is available.² Table 1 lists the meaning of mathematical symbols used in this paper. Table 2 lists the glossary.

2. Related Work

The L2RPN competitions piqued the academic interest in grid topology control with machine learning. Prior research into topology control used linear programming [10, 49], but such methods are too rigid and/or slow to be practical. The first L2RPN competition premiered in 2019. It focused on operating scenarios of the IEEE14-bus network within a specific time frame [28]. The following L2RPN competition was featured at WCCI in 2020 and featured the larger IEEE118-bus network [29]. The next competition at NeurIPS 2020 [27] introduced a robustness track with unplanned outages and an adaptability track with out-of-distribution injection profiles. Later L2RPN competitions focused on trust and sending an alarm signal [26], and the inclusion of batteries [37].

²https://github.com/MatthijsdeJ/GNN_PN_Imitation_Learning

Table 1: Mathematical symbols used in this paper and their meaning.

Notation	Meaning
O	The set of grid objects (i.e., generators, loads, and line endpoints).
S	The set of substations.
\mathbf{x}_u	The features of a GNN model at node $u \in O$.
$\mathbf{h}_{u,k}$	The node embeddings of a GNN model at node $u \in O$ in layer k .
$\mathcal{N}(u)$	The neighbors of node $u \in O$.
W	A weight matrix.
σ	An activation function.
$\mathbf{p} = (0, 1)^{ O }$	The output of a ML model.
$\mathbf{y} = \{0, 1\}^{ O }$	The target of a ML model.
$\alpha = 0.1$	The label weight hyperparameter.
$\mathbf{w} = \{\alpha, 1\}^{ O }$	The label weights for the loss.
$\{\mathbf{p}_s\} \forall s \in S$	A partition of the output vector \mathbf{p} into subvectors \mathbf{p}_s . Sub-vector \mathbf{p}_s corresponds to substation $s \in S$.
$\eta = 0.97$	The activity threshold parameter.
$\theta = 1.0$	The risk threshold parameter, used by various agents.

Graph neural networks have been successfully applied to many tasks of power grid operation, among which power flow estimation [5, 4], optimal power flow computation [31, 11], load shedding [18], outage prediction [13], and stability prediction [30]. For a comprehensive survey on graph reinforcement learning for power grids, we recommend the survey by Hassouna et al. [14].

Several studies investigated GNNs for topology control. Yoon et al. [45] propose a hierarchical actor-critic approach that uses a GNN module to obtain graph embeddings. Their approach won the L2RPN WCCI 2020 challenge. Xu et al. [43] are the first to apply GNNs with graph attention layers for grid topology control. They apply this GNN with a proximal policy optimization approach with an action space searched with monte-carlo tree search. Their approach can, on average, maintain the system for four days in the 2020 NeurIPS L2RPN robustness track. Xu et al. [44] find that a deep reinforcement learning agent which uses features extracted with a GNN trains more quickly and achieve better performance than an agent without.

Table 2: Glossary

Term	Meaning
Busbar Information Asymmetry	An asymmetry in the availability of information of objects on busbars.
Full-network Regime	An environmental regime without statically or randomly disabled lines.
In-distribution Data (ID)	Data with networks that the models are exposed to during training.
Injection	The generators and loads of the environment.
Loading	The ratio of a line’s current over its thermal limit.
Multi-label Binary Classification	A learning task where the target consists of multiple binary values.
N-1 Network	A variation of the default network with a single line disabled.
N-1 Redundancy	The state of the network being resilient to the disablement of any single line.
Object	Generators, loads, and line endpoints in the Grid2Op environment.
Out-of-distribution Data (OOD)	Data with networks that the models are not exposed to during training; used to investigate generalization.
Planned-outage Regime	An environmental regime with statically disabled lines.
Topology Reversal	The periodical resetting of the topology to the default topology.
Topology Vector	The Grid2Op variable that specifies the object-busbar configurations.
Unplanned-outage Regime	An environmental regime with an opponent that randomly disables lines.

Van der Sar et al. [35] propose a hierarchical actor-critic approach with one agent per substations. These agents use graph neural networks blocks, although the details are left unspecified. They apply this approach to the IEEE5-bus network. Qiu et al. [33] propose a method similar to Yoon et al.’s [45] and obtain similar results.

Taha et al. [40] propose a different approach than directly predicting topology actions with GNNs. They use GNNs for grid estimation. These

estimates are then used in grid topology tree search. We will also discuss the approach by Zhao et al. [47], which is relevant because of their focus on generalization. They propose a proximal policy optimization for redispatching that relies on graph embeddings. The graph embeddings are generated by a GraphSAGE model trained with a unsupervised learning task. They find that this graph module can successfully represent out-of-distribution grid changes. Other 2020 NeurIPS L2RPN submissions also used graph neural networks but were not notably successful [27].

Other work did not use graph neural networks. These approaches have mostly used reinforcement learning (RL). Chauhan et al. [2] propose the PowRL framework, which integrates a novel heuristic with an RL approach. They achieved the best results on the legacy 2020 L2RPN robustness track yet. Dorfer et al. [6] adapt the AlphaZero framework [38] for the power grid domain. They achieved top results in the legacy 2020 WCCI L2RPN competition. Pan et al. [32] investigate the vulnerability of RL methods to adversarial attacks. They propose a more robust agent trained adversarially. Subramanian et al. [39] perform an in-depth investigation of a simple agent on a single scenario. Manczak et al. [24] propose a hierarchical RL approach that separates substation and configuration selection.

Imitation learning (IL) has also been applied to the problem of grid topology control. De Jong et al. [15] recently performed the first investigation in IL as a stand-alone method for topology control. They found that both IL and hybrid agents could obtain good performance and inference speed combinations. Prior work on IL used IL as a 'warm start' for RL. Lan et al. [20] first proposed IL to pre-train an RL model for grid control. Binbinchen [8] achieved second place in the 2020 NeurIPS L2RPN submission by expanding this approach. Lehna et al. [22, 21] refined this approach. They introduced topology reversal and a higher-performing N-1 expert agent [22], and a heuristic target topology approach [21]. The winning submission of the 2023 L2RPN competition also included this approach [19].

Other approaches used neither RL nor IL. Zhou et al. [48] use evolutionary strategies to train a model to narrow down the action space. The submission that won both 2020 NeurIPS L2RPN tracks used a similar approach [27]. Although not ML, the expert system developed by Marot et al. has also achieved notoriety [25].

3. Power Grid Setup

3.1. Power Grid

In this study, we experiment on the IEEE14-bus system, displayed in Figure 1. We simulate this system with the `rte_case14_realistic` environment from the Grid2Op library³. The power grid includes fourteen substations, five generators, 11 loads, and 20 power lines. One generator is solar, one nuclear, one wind-based, and two are thermal. The grid is divided into two sides. The high-voltage transmission side contains substations 0 to 4. The low-voltage distribution side contains substations 5 to 13. Lines 15 to 19 model the transformers connecting the two sides of the grid. We adjust the thermal limits to the values specified by Subramanian et al. [39]. This makes the transmission and distribution differences more pronounced and realistic.

We also investigate network variations with single lines disabled. We refer to these as *N-1 networks*. We use the N-1 networks to investigate the ability of agents to operate with line outages and to test the generalization of ML models to out-of-distribution networks.

3.2. Operational Period

The environment features one thousand scenarios, each consisting of 8064 five-minute timesteps. One scenario thus models 28 days. Each scenario features different injection profiles. We split the scenarios into individual days. This daily period better reflects operational periods and emulates beneficial topology reversal [22]. A game-over occurs when the power grid fails to transport sufficient power from generators to loads⁴.

3.3. Action Space

The substations have precisely two busbars in the environment. The topology actions switch *objects*, i.e., generators, loads, and line endpoints, between these busbars. The *topology vector* specifies the busbar attachments of objects. Each index in the vector corresponds to an object. At an index, a value of 1 indicates attachment to the first busbar, 2 indicates attachment to the second busbar, and -1 indicates object disconnection.

³This environment has since been deprecated. Future research should use environment `l2rpn_case14_sandbox`.

⁴Three scenarios were excluded where Grid2Op failed to converge the power flow without agent misoperation. These scenarios were omitted throughout the study.

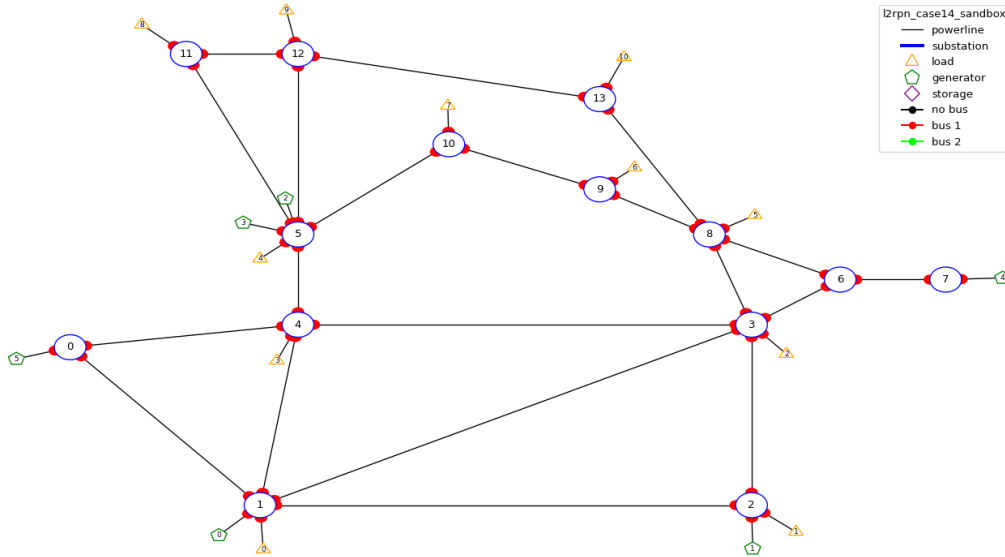


Figure 1: The default state of Grid2Op environment `rte_case14_realistic`.

Actions are limited to a single substation per timestep to reflect real-world timing constraints. Certain substation configurations are invalid (isolated generators or loads) or redundant (configurations mirrored w.r.t. busbars). We use the approach by Subramanian et al. [39] to filter the space of configuration and set-actions. This produces the action space. The procedure is repeated for the different networks to generate the corresponding action spaces (see Subsection 4.1).

3.4. Regimes

We consider three environmental regimes, which represent difficulty levels for grid operation. The *full-network regime* involves the whole network. Lines are statically disabled in the *planned-outage regime*. The *unplanned-outage regime* introduces an opponent that disables lines spontaneously. We use the opponent specified by Manczak et al. [24]. The opponent disables a randomly selected line for four hours twice a day. A cooldown period ensures that outages are separated by at least an hour.

Table 3: The number of datapoints in the datasets and train/val/test sets.

	Train	Val	Test
ID	196,477	26,228	59,150
OOD	41,788 ^a	5,690 ^a	12,724

^a These datapoints are used to train a model to estimate an upper bound to generalization (see Sec. 4.8).

4. Methods

4.1. Datasets

We use the data generated with the two expert agents from our previous study [15]. The first agent is the *greedy agent*, which decreases the line loading greedily. The second agent is the *N-1 agent*, which pursues topologies that are N-1 redundant. We found that the N-1 agent performed superiorly to the Greedy agent in settings with and without outages. Both agents have an activity threshold, below which do-nothing actions are taken automatically. State-action pairs with such do-nothing actions or from unsuccessful days are excluded. Do-nothing actions above this threshold are included.

We create two datasets. First, a *in-distribution* (ID) dataset containing networks on which the models are trained and evaluated. This dataset was used in our previous study [15]. This dataset combines the data from the greedy agent and the N-1 agent. The data from the N-1 agent on the full network is used. The data from the greedy agent on a subset of the N-1 networks is used. These are the N-1 networks with lines 0, 2, 4, 5, 6, and 12 disabled, which the greedy agent can operate well [15].

Second, an *out-of-distribution* (OOD) dataset, which is used to investigate generalization. This dataset comprises data from the greedy agent on the N-1 networks with lines 1 and 3 disabled.

On both datasets, we split the datapoints into 70/10/20 train/validation/test sets based on their scenario. The sizes of the partitions are listed in Table 3. In this paper, ID or OOD networks refer to the networks in either the ID or OOD datasets. ID or OOD outages refer to the outages present in either ID or OOD networks.

4.2. Datapoints

Each datapoint includes the features per object, the topology vector, and the expert action. The features for each object type are listed in Table 4. The

object features are normalized. If a line is disabled, its endpoint features are zero-imputed, and the corresponding topology vector values are -1. Actions are converted from a set-action format into a switch-action format. Thus, actions are represented by a vector with a length of the topology vector. Each index indicates whether the corresponding object is switched between busbars (a value of 1) or not (a value of 0). This presents a **multi-label binary classification task**.

4.3. FCNN

The fully connected neural network (FCNN) consists of an input layer, multiple hidden layers, and an output layer. The input vector is obtained by flattening the input features into a vector and concatenating the topology vector. The hidden layers use the ReLU activation function. The output layer uses the sigmoid activation function to constrain the output to the $(0, 1)$ range. The output vector has the length of the topology vector, so one value $p_u \in (0, 1)$ is predicted per node u .

4.4. Homogeneous GNN

Applying a graph neural network to the power grid requires a graph representation of the power grid. We represent the grid objects as nodes. We connect nodes if the corresponding objects are attached to the same busbar or are corresponding line endpoints. We call this graph representation *homogeneous* as it does not consider edge types. We call the associated GNN the *HomGNN*. Figures 2a and 2b display an example grid and its homogeneous representation.

Different types of grid objects have different features (see Table 4). We use multiple two-layer perceptrons to embed the varying object features into

Table 4: Features per object type.

Generator/Load	Line endpoint	
Active Production/Load	Active Power Flow	Current flow
Reactive Production/Load	Reactive Power Flow	Loading (ρ)
Voltage Magnitude	Voltage Magnitude	Thermal Limit

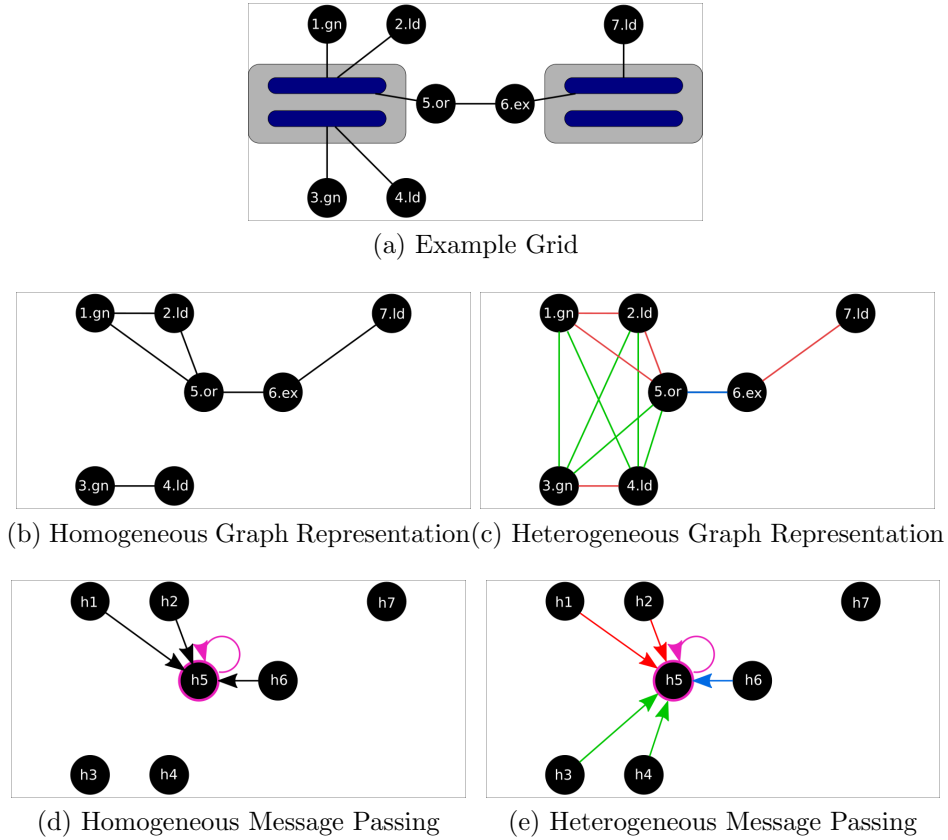


Figure 2: **a**: An example grid consisting of two substations and seven objects. Note that this grid is unrealistic, as real power grids should not be split. **b**: The homogeneous graph representation of that grid. **c**: The heterogeneous graph representation of that grid, where edge colors indicate edge types. **d**: Message passing towards node 5 in the homogeneous model. The purple reflective edge is added to reflect self-weights. **e**: Message passing towards node 5 in the heterogeneous model, where edge colors indicate message types.

a common embedding:

$$\mathbf{h}_{u,0} = \begin{cases} \text{MLP}_{gen}(\mathbf{x}_u) & \text{node } u \text{ represents a generator} \\ \text{MLP}_{load}(\mathbf{x}_u) & \text{node } u \text{ represents a load} \\ \text{MLP}_{line}(\mathbf{x}_u) & \text{node } u \text{ represents a line endpoint,} \end{cases}$$

where $\mathbf{h}_{u,0}$ and \mathbf{x}_u are, respectively, the initial node embedding and the features of node u . The embeddings of subsequent layers are computed with

the message passing rule [36]:

$$\mathbf{h}_{u,k+1} = \sigma(W_{self,k}\mathbf{h}_{u,k} + W_{neighbor,k} \sum_{v \in \mathcal{N}(u)} \mathbf{h}_{v,k} + \mathbf{b}_k),$$

where $\mathbf{h}_{u,k}$ is the embedding for node u in layer k , σ is the activation function, $W_{self,k}$ and $W_{neighbor,k}$ are the self and neighbor weights in layer k , $\mathcal{N}(u)$ is the neighborhood of node u , and \mathbf{b}_k is the bias term. Figure 2d displays an example of homogeneous message passing. The activation function σ is the ReLU function in all but the final layer. The final layer uses the sigmoid activation function and outputs one value. Thus, the model predicts one value $p_u \in (0, 1)$ per node u .

4.5. Busbar Information Asymmetry

The aforementioned graph neural network formulation has a problem. Each node’s output specifies whether to switch the corresponding object between busbars. However, messages from objects on the current busbar are passed, while messages from the objects on the other busbar are not. We call this the *busbar information asymmetry*. This is intuitively problematic as a switching decision requires information about the other busbar. This also decreases the model’s expressiveness. Objects at the same substation but on different busbars and objects at entirely different substations cannot be distinguished. Moreover, the absence of inter-busbar connections also decreases the graph’s connectivity. This can result in longer paths that may require deeper GNNs.

4.6. Heterogeneous GNN

Our solution is to represent the grid with a *heterogeneous* graph representation. The associated GNN is called the *HetGNN*. This heterogeneous representation features three edge types: one for objects on the same busbar, one for objects on the other busbar (but at the same substation), and one for corresponding line endpoints. This is displayed in Figure 2c. The message passing rule is adapted to consider a weight and neighborhood aggregation per edge type:

$$\mathbf{h}_{u,k+1} = \sigma(W_{self,k}\mathbf{h}_{u,k} + W_{same,k} \sum_{v \in \mathcal{N}_{same}(u)} \mathbf{h}_{v,k} + W_{other,k} \sum_{v \in \mathcal{N}_{other}(u)} \mathbf{h}_{v,k} + W_{line,k}\mathbf{h}_{line,k} + \mathbf{b}_k),$$

where \mathcal{N}_{same} and \mathcal{N}_{other} denote the neighborhoods of objects on the same and other busbar, respectively. The $W_{line,k}\mathbf{h}_{line,k}$ term represents the addition of the embedding of a node connected by a power line. It is therefore omitted for nodes that do not represent line endpoints. Figure 2e displays an example of heterogeneous message passing.

4.7. Optimization & Postprocessing

The weights are initialized using a normal distribution, with the standard deviation set as a tuned hyperparameter. We use the Adam optimizer to minimize a label-weighted binary cross-entropy loss, defined as:

$$L = \text{mean}(-\mathbf{w}(\mathbf{y} \log(\mathbf{p}) + (\mathbf{1} - \mathbf{y}) \log(\mathbf{1} - \mathbf{p}))),$$

where \mathbf{w} , \mathbf{y} , and \mathbf{p} denote the label weight, target, and prediction vectors, respectively. We introduce label weights to prevent the prediction vectors from collapsing to zeros. This occurs as the majority of target values are zero. A lower label weight $0 < \alpha < 1$ is assigned to labels that do not correspond to objects at either the target or predicted substation:

$$w_i = \begin{cases} 1 & \text{object } i \text{ corresponds to the target substation} \\ 1 & \text{object } i \text{ corresponds to the predicted substation} \\ \alpha & \text{otherwise} \end{cases} \quad \forall w_i \in \mathbf{w}.$$

There is no target substation if the target action is a do-nothing action. The predicted action is classified as a do-nothing action, without a predicted substation, if all predictions $p_i \in \mathbf{p}$ do not exceed 0.5. Otherwise, the predicted substation is the substation where the predictions \mathbf{p}_s at that substation $s \in S$ maximize

$$\sum_{p_i \in \mathbf{p}_s} \max(p_i - 0.5, 0).$$

Each value in the prediction vector represents whether to switch the corresponding object. However, not every prediction vector corresponds to an action in the filtered action space (see Sec. 3.3). We apply a postprocessing step that replaces the model’s prediction \mathbf{p} with the nearest action. This postprocessing step is applied during validation, testing, and inference but not during training.

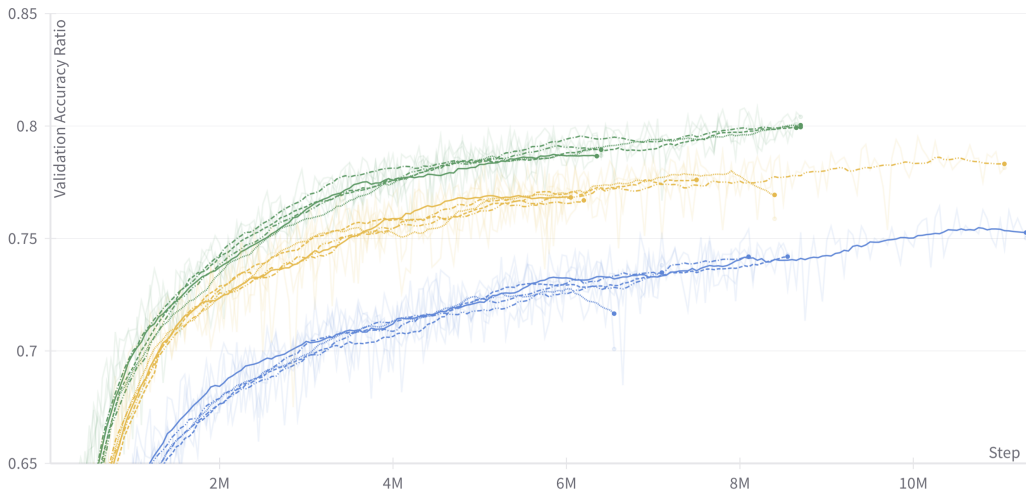


Figure 3: The training curves of the five models per model type. Green lines show the HetGNNs, yellow lines the FCNNs, and blue lines the HomGNNs.

4.8. Hyperparameter Tuning & Training

The hyperparameters were tuned with two iterations of hyperparameter sweeps. This procedure was repeated for the three model types. The first sweep narrowed the hyperparameter ranges. It covered wide parameter ranges and trained for a few epochs with strict early stopping. The second sweep covered narrower ranges and trained with more epochs and less strict early stopping. All sweeps use random search with Hyperband early termination (distinct from early stopping). Hyperband early termination terminated unpromising runs early. Table 5 describes all final hyperparameter values, the second sweep ranges, and additional clarification where necessary.

Five models were trained per model type, each with different weight initializations. Each training run lasted for 100 epochs unless stopped early. Runs were terminated early if the highest validation accuracy did not increase in 20 evaluations. The validation accuracy was calculated every 50,000 iterations. The training curves are displayed in Figure 3. Finally, we trained five heterogeneous GNNs on the OOD data to contrast the models’ generalization performance. These are referred to as *OOD-GNNs*.

4.9. Imitation Learning Agents

The ML models are applied to the environment. They can be applied directly or combined with simulation. The *naive* agent executes a model’s

Table 5: Hyperparameters and their final sweep ranges for both the FCNNs and GNNs.

Hyperparameter	FCNN Value	FCNN Range	GNN Value ^a	GNN Range ^a
#Hidden Layers	4	(1, 5)	8	(2, 12)
#Hidden Nodes	230	(32, 256)	180	(32, 256)
Batch Size	64	(32, 128)	64	(32, 128)
Learning Rate	7E-4	(e^{-9} , e^{-5})	2E-4	(e^{-9} , e^{-5})
Weight Decay	0 ^b	(e^{-9} , e^{-2})	0 ^b	(e^{-9} , e^{-2})
Weight Init. σ	5	($e^{-0.5}$, $e^{1.5}$)	5	($e^{-0.5}$, $e^{1.5}$)
Label Weight α	0.1	- ^c	0.1	- ^c
ReLU neg. slope	0.1	- ^d	0.1	- ^d

^a Hyperparameter tuning was performed independently for both the HomGNN and HetGNN. However, the results were sufficiently similar. Hence, the same ranges and final values were selected. ^b Weight decay was set to zero after observing that the best runs had values near the lower limit. Subsequent runs with a weight decay of zero performed better. ^c We experimented with label weight α values when introducing label weighting. Label weights were not included in the hyperparameter sweeps. ^d The ReLU negative slope parameter was not tuned.

predicted action directly. We observe that this agent occasionally fails by predicting a singular erroneous action. The *verify* agent addresses this by verifying predicted actions with simulation. The predicted action is simulated. A do-nothing action is selected if the simulated line loadings are increased beyond the thermal limit. We also consider hybrid agents. The *verify+greedy* agent normally functions as the verify agent, but switches to the greedy agent if a line breaches the thermal limit. The *verify+N-1* agent functions similarly but with the N-1 agent. Each agent also uses the activity threshold used by the expert agents [15].

5. Results

5.1. Supervised Learning

Table 6 lists the accuracies of the different models on the various data partitions and the ID/OOD network groups. Figure 4 shows the test accuracies of the models on both datasets. On the ID dataset (rows 1 to 3), the

Table 6: The accuracies of the different models on the different combinations of data partitions and ID/OOD network sets. Numbers indicate the mean and standard deviation of accuracy for the five models. Remember that the data partitions are split by scenario.

#	(%)	FCNN	HomGNN	HetGNN	OOD-GNN
1	ID Train	79.2±0.9	75.2±0.9	83.2±1.4	-
2	ID Val	78.6±0.5	75.1±0.8	80.2±0.6	-
3	ID Test	76.6±0.6	73.0±0.6	78.5±0.8	-
4	Raw ID Test ^a	73.9±0.6	67.9±0.6	74.7±0.5	-
5	Default ID Test ^b	94.5±0.9	94.2±0.4	95.3±0.3	-
6	Split ID Test ^c	61.3±0.9	54.8±1.2	64.1±1.2	-
7	OOD Train	35.0±0.9	63.4±1.1	67.9±0.7	86.0±0.6
8	OOD Val	37.3±0.4	65.6±0.6	69.3±0.7	83.7±0.2
9	OOD Test	34.7±0.7	61.1±0.7	65.1±0.7	80.7±0.4

^a This lists the accuracy without the postprocessing step described in Sec. 4.7. ^b These datapoints represent the default topology, i.e., without split substations. ^c These datapoints represent non-default topologies, i.e., with split substations.

accuracies remain limited to approximately 80%. On each split, the HetGNN achieves the highest accuracy, followed by the FCNN and, lastly, the HomGNN. Each model type shows a tiny drop in accuracy between the train, validation, and test sets, indicating slight overfitting. Row 4 displays that accuracy drops slightly without the postprocessing step described in Sec. 4.7.

The default topology appears frequently in the ID dataset, comprising 46% of the test set. In this topology, all objects are attached to the same busbar. This avoids the busbar asymmetry problem and consequently negates the theoretical advantage of the HetGNN over the HomGNN. As shown in row 5, the accuracies on the standard topology are relatively similar. As shown in row 6, the accuracies vary considerably between topologies with split busbars.

The GNNs obtain far higher accuracies on the OOD dataset than the FCNNs (rows 7 to 9). The HetGNNs also obtain higher accuracies than the HomGNNs. However, the performance of either the HomGNN or the HetGNN on the OOD dataset is still substantially lower than models trained on OOD data (column 'OOD-GNN').

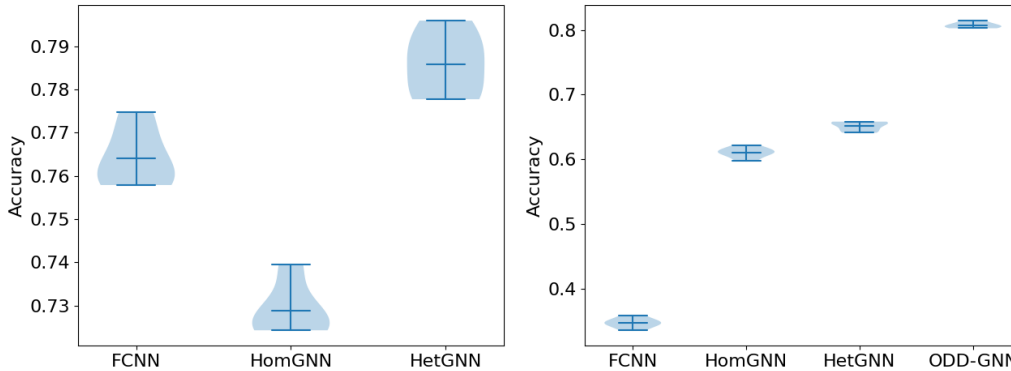


Figure 4: The test accuracies of the model types on the ID dataset set (left) and OOD dataset (right). The ranges indicate the maximum and minimum accuracy.

5.2. Error Analysis

We repeated the error analysis previously performed on the FCNN [15] to the two types of GNN models. We again find that the class imbalance and class overlap play a role in the limited accuracy. Figure 5 shows that both GNN types predict infrequent classes disproportionately infrequently. We investigated pairs of classes that were often confused, i.e., pairs of classes that were often mistaken for one another in prediction. Figure 6 shows that the errors of frequently confused classes are in overlapping regions.

Inspection of the nearest neighbors supports the notion that the class overlap contributes to low accuracy. We applied one of the HetGNNs to a subset of 2,500 validation data points from the full network. The accuracy over the data points whose nearest neighbor is in the same class is 92.97%, but only 44.44% for those whose nearest neighbor is in another class. Other models showed similar results.

5.3. Graph Smoothness

The tendency of graph neural networks to suffer from oversmoothing is well-documented [3, 23]. We compute the mean average distance (MAD) values to measure graph smoothness [3]. MAD values quantify the similarity of node embeddings. Small MAD values indicate that node embeddings are similar and, thus, that the graph is smooth.

The MAD values are computed between neighbor nodes over the first 1000 validation datapoints. Figure 7 shows the MAD values between the

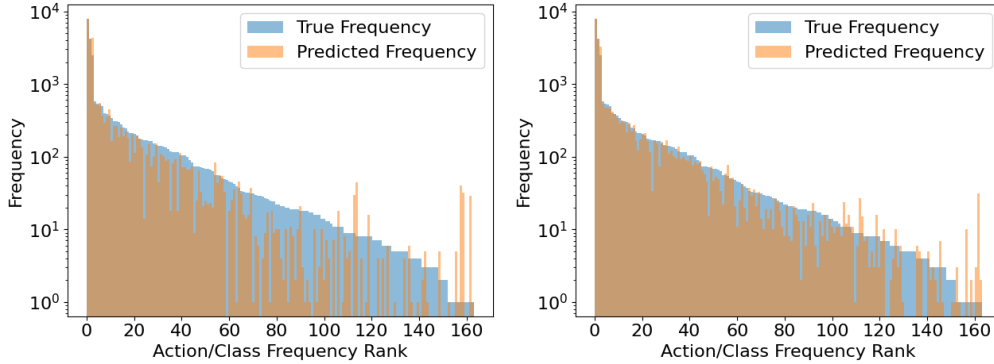


Figure 5: The log-distributions of the classes in the ID validation set. Overlaid is the frequency by which the model predicts that class (left: HomGNN, right: HetGNN). The non-overlapping blue areas at the tails of the distributions indicate that the models predict rare classes disproportionately infrequently. This finding is consistent among the models.

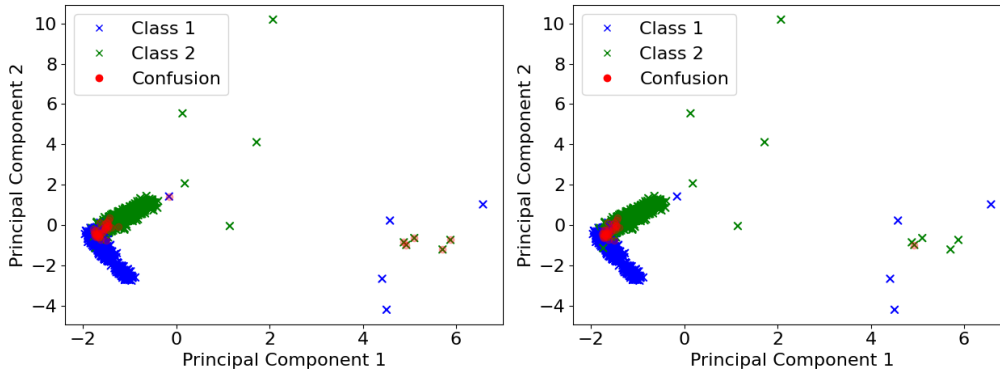


Figure 6: The datapoints of two classes that are most often confused, for the N-1 network with line 0 disabled. The datapoints are projected on the first two principal components. The datapoints confused by the models (left: HomGNN, right: HetGNN) are overlaid in red. As visible, the datapoints in the overlapping region are confused. This finding is consistent among the models and confused classes.

various layers. As visible, the MAD values in the middle GNN layers are consistently higher in the HetGNN than in the HomGNN. This suggests that the heterogeneous representation leads to a less smooth local embedding. This finding is consistent among the models.

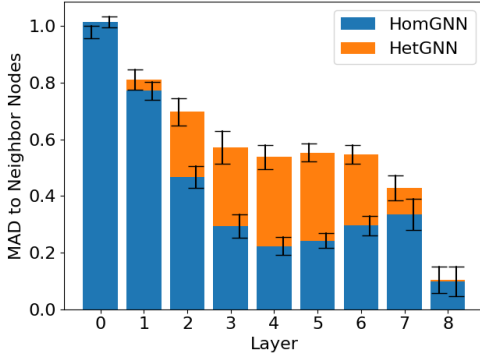


Figure 7: The average neighbor MAD values per layer of a HomGNN and a HetGNN. As visible, the HomGNN has far lower neighbor MAD values in the middle layers. Layers 0 and 8 indicate the neighbor MAD values before and after the message-passing layers. Error bars indicate the standard deviations over the 1000 datapoints.

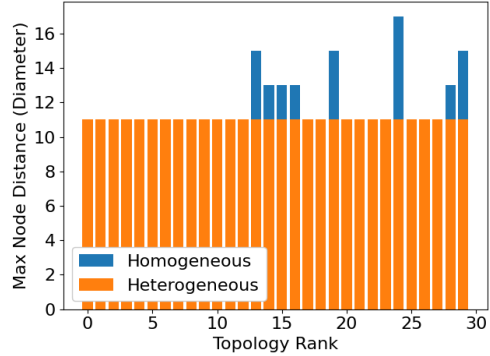


Figure 8: The diameter of the 25 most common topologies. The diameter of the heterogeneous graph representation is invariant to busbar reconfiguration.

5.4. Graph Diameter

We mentioned that the heterogeneous graph representation can lead to shorter paths. We measure this by the diameter, i.e., the shortest path length between the two most distant nodes. We calculate the diameter by finding the lowest exponent of the adjacency matrix that produces a matrix without zero entries [7]. The diameters of the 25 most common topologies are shown in Figure 8. As visible, the heterogeneous graph representation infrequently leads to a shorter diameter.

5.5. Simulation Performance

Table 7 shows the days completed by the various agents in the different settings. The 'Full Network' column describes the setting without outages. The 'ID Outages' describes a setting with an opponent that causes random outages present in the ID dataset (see Sec. 4.1). The 'OOD Outages' describes a setting with an opponent that causes random outages present in the OOD dataset.

The agents can be ordered by performance: Do-Nothing < Naive < Verify < Greedy Hybrid < N-1 Hybrid. The naive agents (rows 4 to 6) and verify agents (rows 8 to 10) come close to the performance of the N-1 expert agents

Table 7: The percentage of days completed by agents in various regimes. The agents were evaluated on the test scenarios.

#	Agent Type	Model Type	Full Network	ID Outages ^a	OOD Outages ^a
1	Do-Nothing		59.80	46.57±0.17	54.20±0.3
2	Greedy		99.73 ^b	81.79±1.02	86.30±1.12
3	N-1		100.00 ^b	92.39±0.24	93.08±0.48
4	Naive ^c	FCNN	96.27±0.90	86.33±0.90	83.74±1.13
5		HomGNN	95.39 ± 0.29	85.34±0.97	86.06±0.60
6		HetGNN	96.69 ± 0.23	87.76±0.57	88.02±1.78
7		OOD-GNN	-	-	92.72±0.72
8	Verify ^c	FCNN	98.95±0.19	89.62±0.57	87.93±0.73
9		HomGNN	98.82±0.14	88.51±0.60	89.27±0.80
10		HetGNN	99.35±0.05	90.89±0.36	91.46±0.86
11		OOD-GNN	-	-	95.01±0.48
12	Greedy _c Hybrid	FCNN	99.85±0.04	93.76±0.16	93.23±0.26
13		HomGNN	99.78±0.05	93.44±0.41	94.68±0.28
14		HetGNN	99.88±0.03	93.88±0.34	94.74±0.67
15		OOD-GNN	-	-	97.82±0.13
16	N-1 Hybrid ^c	FCNN	99.97±0.02	95.17±0.18	94.49±0.19
17		HomGNN	100.00±0.00	94.72±0.15	95.69±0.55
18		HetGNN	100.00±0.00	95.08±0.35	95.41±0.80
19		OOD-GNN	-	-	98.52±0.11

^a These results are averaged over five seeds of outages randomly disabled by an opponent. ^b These results were computed over all scenarios as part of data analysis. ^c These results are averaged over the five different models. ^{a∩c} In the intersection, results are averaged over five different runs, each with a different model and random outages.

(row 3). The hybrid agents (rows 12 to 14, and 16 to 18) can match the N-1 expert agents.

On the setting with no or ID outages (columns 'Full Network' and 'ID Outages') the HetGNN network consistently performs best, followed by the FCNN and, finally, the HomGNN (rows 4 to 6, and 8 to 10). Additional simulation reduces or nullifies the differences (rows 12 to 14, and 16 to 18).

On the setting with OOD outages (column 'OOD Outages'), the GNNs

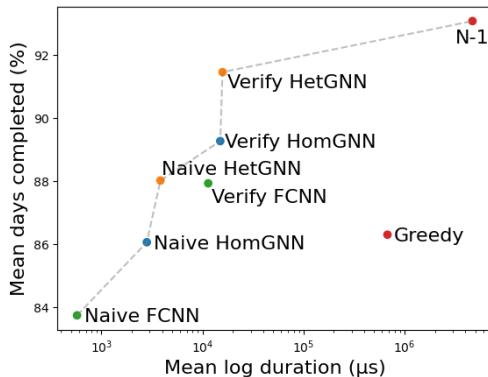


Figure 9: The performance and inference duration for the agents on the setting with OOD outages. The combinations of speed and performance of the imitation learning agents are favorable. All GNN agents are on the Pareto front (dashed line). The GNN models are somewhat slower than the FCNN models.

Table 8: Inference durations of various agents. The hybrid models all use the FCNN. The differences between model types for the hybrid agents are relatively insignificant.

Agent	Duration (μs)
Greedy	6.77E5
N-1	4.70E6
Naive FCNN	5.74E2
Naive HomGNN	2.81E3
Naive HetGNN	3.84E3
Verify FCNN	1.14E4
Verify HomGNN	1.50E4
Verify HetGNN	1.58E4

outperform the FCNN (rows 4 to 6, and 8 to 10). However, additional simulation also decreases this effect (rows 12 to 14, and 16 to 18). Furthermore, the performance of the models trained on the ID dataset remains substantially lower than models trained on OOD dataset (rows 7 and 11), even with additional simulation (rows 15 and 19).

5.6. Efficiency

Finally, we consider the inference speed of the different agents. The inference speed was measured on an Apple M1 CPU with minimal background processes on the first fifty validation scenarios. Table 8 lists the durations per model type and agent. Figure 9 plots these values against the agent’s performance on the full-network topology. The GNNs, particularly the HetGNNs, are considerably slower than the FCNNs. However, these differences are small relative to the simulation times of the expert agents, which are orders of magnitude higher. Most importantly, all GNN agents have a favorable combination of speed and performance.

6. Discussion

The heterogeneous GNN consistently performs best, followed by the FCNN, and lastly, the homogeneous GNN. This is true for both the accuracy and grid operation. The superiority of the HetGNN to the FCNN indicates that GNNs can exploit the graph structure better. The inferiority of the HomGNN can be attributed to the busbar asymmetry problem. However, smoother graphs and longer path lengths might also play a role. The HetGNN’s coarser graphs can be attributed to the more diverse edge representation. The GNNs take considerably longer to evaluate than the FCNNs, although this difference is very tiny compared to the expert agents.

The GNNs achieve far higher accuracy than the FCNNs on the OOD networks. This is also reflected in the simulation performance, although the effect is smaller. Although GNNs show a superior ability to generalize to OOD networks, they still perform considerably worse than GNNs trained on these networks.

There seemed to be a limit to the accuracy of the trained models. This can be attributed to class imbalance and class overlap. We hypothesize that the class overlap originates from the Grid2Op `simulate` function. It is possible that identical network states have diverging forecasts and consequently diverging actions. The limited accuracy does not stop the ML models from successfully completing many of the grid operation days. The naive ML models come close to the performance of the expert agents. The hybrid agents can match them.

Hybrid agents can outperform expert agents in specific settings, which is surprising. We hypothesize that this results from omitting the state-action pairs from failed runs. The model bias towards frequent actions might also result in more robust topologies.

An interesting effect is that model differences are more pronounced in accuracy than simulation performance. Similarly, the limited accuracy does not stop the models from operating the grid well. We have two explanations for this. Firstly, a misprediction does not necessarily lead to a game-over. This is probably particularly true in regions with class overlap. Secondly, difficult days led to the generation of many relatively uncommon datapoints. Failure to predict many such datapoints would consequently affect the completion of only few days.

7. Future Work

Our findings indicate the promise of fully graphical neural networks for topology control methods. However, further research is necessary to establish this. Future work should compare fully GNN models with models that only use GNNs for feature extraction. Similarly, the heterogeneous graph representation should be introduced into other approaches. Moreover, it would be good to apply these methods in a reinforcement learning framework.

Further efforts are likely also necessary to scale this approach to larger grids. Fully GNN models might require very deep GNNs to model large graphs. Very deep GNNs are associated with additional challenges [46]. Future research could focus on methods to downsample grid graph representations, e.g., through trainable graph pooling [12]. Alternatively, it might be beneficial to combine GNN layers and other layers to capture long-range patterns.

The imitation learning approach used here can also be developed further. Our approach suffers from *distribution shift*, a compounding divergence between the behavior of the ML and the expert agent [1]. More advanced IL frameworks, such as DAgger, address this [34]. Investigating other expert agents and developing an improved dataset would also be valuable.

Finally, the generalization capabilities of graph neural networks should be studied more extensively. Future studies should investigate how factors such as the diversity of training data and differences between the ID and OOD data affect generalization.

8. Statements

8.1. CRediT authorship contribution statement

Matthijs de Jong: Methodology, Software, Formal Analysis, Investigation, Data Curation, Writing - Original Draft, Visualization. **Jan Viebahn**: Conceptualization, Methodology, Resources, Writing - Review & Editing, Supervision, Project Administration. **Yuliya Shapovalova**: Methodology, Resources, Writing - Review & Editing, Supervision.

8.2. Declaration of competing interest

The authors declare the following financial interests/personal relationships which may be considered as potential competing interest: Jan Viebahn and Matthijs de Jong reports financial support was provided by TenneT TSO BV. Yuliya Shapovalova declares that she has no such interests.

8.3. Acknowledgements

Special thanks to Mohamed Hassouna from Fraunhofer Society for providing valuable feedback. This work is supported by Graph Neural Networks for Grid Control (GNN4GC) founded by the Federal Ministry for Economic Affairs and Climate Action Germany under the funding code 03EI6117A.

8.4. Funding

This research did not receive any specific grant from funding agencies in the public, commercial, or not-for-profit sectors.

8.5. Code & Data Availability

Our code ² and data [16] are publicly available.

References

- [1] Belkhale, S., Cui, Y., Sadigh, D.: Data quality in imitation learning. *Advances in Neural Information Processing Systems* **36** (2024)
- [2] Chauhan, A., Baranwal, M., Basumatary, A.: PowRL: a reinforcement learning framework for robust management of power networks. *AAAI'23/IAAI'23/EAAI'23*, AAAI Press (2023). <https://doi.org/10.1609/aaai.v37i12.26724>
- [3] Chen, D., Lin, Y., Li, W., Li, P., Zhou, J., Sun, X.: Measuring and relieving the over-smoothing problem for graph neural networks from the topological view. *Proceedings of the AAAI Conference on Artificial Intelligence* **34**, 3438–3445 (04 2020). <https://doi.org/10.1609/aaai.v34i04.5747>
- [4] Donon, B., Clément, R., Donnot, B., Marot, A., Guyon, I., Schoenauer, M.: Neural networks for power flow: Graph neural solver. *Electric Power Systems Research* **189**, 106547 (2020). <https://doi.org/https://doi.org/10.1016/j.epsr.2020.106547>
- [5] Donon, B., Donnot, B., Guyon, I., Marot, A.: Graph neural solver for power systems. In: *2019 International Joint Conference on Neural Networks (IJCNN)*. pp. 1–8 (2019). <https://doi.org/10.1109/IJCNN.2019.8851855>

- [6] Dorfer, M., Fuxjäger, A., Kozak, K., Blies, P., Wasserer, M.: Power grid congestion management via topology optimization with AlphaZero (11 2022). <https://doi.org/10.48550/arXiv.2211.05612>
- [7] Duncan, A.J.: Powers of the adjacency matrix and the walk matrix (2004), <https://api.semanticscholar.org/CorpusID:127195893>
- [8] EI Innovation Lab, Huawei Cloud, Huawei Technologies: NeurIPS competition 2020: Learning to run a power network (L2RPN) - robustness track. https://github.com/AsprinChina/L2RPN_NIPS_2020_a_PPO_Solution (2020), [Accessed: 24-06-2024]
- [9] ENTSO-E: European electricity transmission grids and the energy transition (2021), https://eepublicdownloads.entsoe.eu/clean-documents/mc-documents/210414_Financeability.pdf
- [10] Fisher, E.B., O’Neill, R.P., Ferris, M.C.: Optimal transmission switching. *IEEE Transactions on Power Systems* **23**(3), 1346–1355 (2008). <https://doi.org/10.1109/TPWRS.2008.922256>
- [11] Gao, M., Yu, J., Yang, Z., Zhao, J.: A physics-guided graph convolution neural network for optimal power flow. *IEEE Transactions on Power Systems* **39**(1), 380–390 (2024). <https://doi.org/10.1109/TPWRS.2023.3238377>
- [12] Grattarola, D., Zambon, D., Bianchi, F.M., Alippi, C.: Understanding pooling in graph neural networks. *IEEE Transactions on Neural Networks and Learning Systems* **35**(2), 2708–2718 (2024). <https://doi.org/10.1109/TNNLS.2022.3190922>
- [13] Hansen, J.B., Anfinson, S.N., Bianchi, F.M.: Power flow balancing with decentralized graph neural networks. *IEEE Transactions on Power Systems* **38**(3), 2423–2433 (2023). <https://doi.org/10.1109/TPWRS.2022.3195301>
- [14] Hassouna, M., Holzhüter, C., Lytaev, P., Thomas, J., Sick, B., Scholz, C.: Graph reinforcement learning for power grids: A comprehensive survey (2024), <https://arxiv.org/abs/2407.04522>

- [15] de Jong, M., Viebahn, J., Shapovalova, Y.: Imitation learning for intraday power grid operation through topology actions. In: Springer Communications in Computer and Information Science. To appear in ECML-PKDD 2024 post-workshop proceedings. Pre-print available: <https://arxiv.org/abs/2407.19865>
- [16] de Jong, M., Viebahn, J., Shapovalova, Y.: Imitation learning topology control dataset (2024). <https://doi.org/10.17632/w82pscwxgm.1>, <https://doi.org/10.17632/w82pscwxgm.1>
- [17] Kelly, A., O’Sullivan, A., de Mars, P., Marot, A.: Reinforcement learning for electricity network operation (2020). <https://doi.org/10.48550/arXiv.2003.07339>
- [18] Kim, C., Kim, K., Balaprakash, P., Anitescu, M.: Graph convolutional neural networks for optimal load shedding under line contingency. In: 2019 IEEE Power & Energy Society General Meeting (PESGM). pp. 1–5 (2019). <https://doi.org/10.1109/PESGM40551.2019.8973468>
- [19] La Javaness R&D: How we built the winning real time autonomous agent for power grid management in the L2RPN challenge 2023. <https://lajavaness.medium.com/how-we-built-the-winning-real-time-autonomous-agent-for-power-grid-management-in-the-l2rpn-41ab3cfaddbd> (2024), [Accessed: 24-06-2024]
- [20] Lan, T., Duan, J., Zhang, B., Shi, D., Wang, Z., Diao, R., Zhang, X.: AI-based autonomous line flow control via topology adjustment for maximizing time-series ATCs. In: 2020 IEEE Power & Energy Society General Meeting (PESGM). pp. 1–5 (2020). <https://doi.org/10.1109/PESGM41954.2020.9281518>
- [21] Lehna, M., Holzhüter, C., Tomforde, S., Scholz, C.: HUGO – highlighting unseen grid options: Combining deep reinforcement learning with a heuristic target topology approach. *Sustainable Energy, Grids and Networks* **39**, 101510 (2024). <https://doi.org/10.1016/j.segan.2024.101510>
- [22] Lehna, M., Viebahn, J., Marot, A., Tomforde, S., Scholz, C.: Managing power grids through topology actions: A comparative study between advanced rule-based and reinforcement learning agents. *Energy and AI* **14**, 100276 (2023). <https://doi.org/10.1016/j.egyai.2023.100276>

- [23] Li, Q., Han, Z., Wu, X.M.: Deeper insights into graph convolutional networks for semi-supervised learning. In: Proceedings of the Thirty-Second AAAI Conference on Artificial Intelligence and Thirtieth Innovative Applications of Artificial Intelligence Conference and Eighth AAAI Symposium on Educational Advances in Artificial Intelligence. AAAI'18/IAAI'18/EAAI'18, AAAI Press (2018). <https://doi.org/10.1609/aaai.v32i1.11604>
- [24] Manczak, B., Viebahn, J., van Hoof, H.: Hierarchical reinforcement learning for power network topology control (2023). <https://doi.org/10.48550/arXiv.2311.02129>
- [25] Marot, A., Donnot, B., Tazi, S., Panciatici, P.: Expert system for topological remedial action discovery in smart grids. pp. 43 (6 pp.)–43 (6 pp.) (01 2018). <https://doi.org/10.1049/cp.2018.1875>
- [26] Marot, A., Donnot, B., Chaouache, K., Kelly, A., Huang, Q., Hossain, R.R., Cremer, J.L.: Learning to run a power network with trust. *Electric Power Systems Research* **212**, 108487 (2022). <https://doi.org/10.1016/j.epsr.2022.108487>
- [27] Marot, A., Donnot, B., Dulac-Arnold, G., Kelly, A., O'Sullivan, A., Viebahn, J., Awad, M., Guyon, I., Panciatici, P., Romero, C.: Learning to run a power network challenge: a retrospective analysis (03 2021). <https://doi.org/10.48550/arXiv.2103.03104>
- [28] Marot, A., Donnot, B., Romero, C., Donon, B., Lerousseau, M., Veyrin-Forrer, L., Guyon, I.: Learning to run a power network challenge for training topology controllers. *Electric Power Systems Research* **189**, 106635 (2020). <https://doi.org/10.1016/j.epsr.2020.106635>
- [29] Marot, A., Guyon, I.: L2RPN WCCI 2020 competition. <https://competitions.codalab.org/competitions/24902>
- [30] Nauck, C., Lindner, M., Schürholt, K., Zhang, H., Schultz, P., Kurths, J., Isenhardt, I., Hellmann, F.: Predicting basin stability of power grids using graph neural networks. *New Journal of Physics* **24**(4), 043041 (apr 2022). <https://doi.org/10.1088/1367-2630/ac54c9>
- [31] Owerko, D., Gama, F., Ribeiro, A.: Optimal power flow using graph neural networks. In: ICASSP 2020 - 2020 IEEE International Conference

- on Acoustics, Speech and Signal Processing (ICASSP). pp. 5930–5934 (2020). <https://doi.org/10.1109/ICASSP40776.2020.9053140>
- [32] Pan, A., Lee, Y., Zhang, H., Chen, Y., Shi, Y.: Improving robustness of reinforcement learning for power system control with adversarial training (2021). <https://doi.org/10.48550/arXiv.2110.08956>
- [33] Qiu, Z., Zhao, Y., Shi, W., Su, F., Zhu, Z.: Distribution network topology control using attention mechanism-based deep reinforcement learning. In: 2022 4th International Conference on Electrical Engineering and Control Technologies (CEEECT). pp. 55–60 (2022). <https://doi.org/10.1109/CEEECT55960.2022.10030642>
- [34] Ross, S., Gordon, G., Bagnell, D.: A reduction of imitation learning and structured prediction to no-regret online learning. In: Gordon, G., Dunson, D., Dudík, M. (eds.) Proceedings of the Fourteenth International Conference on Artificial Intelligence and Statistics. Proceedings of Machine Learning Research, vol. 15, pp. 627–635. PMLR, Fort Lauderdale, FL, USA (11–13 Apr 2011), <https://proceedings.mlr.press/v15/ross11a.html>
- [35] van der Sar, E., Zocca, A., Bhulai, S.: Multi-agent reinforcement learning for power grid topology optimization (2023), <https://arxiv.org/abs/2310.02605>
- [36] Scarselli, F., Gori, M., Tsoi, A.C., Hagenbuchner, M., Monfardini, G.: The graph neural network model. *IEEE Transactions on Neural Networks* **20**(1), 61–80 (2009). <https://doi.org/10.1109/TNN.2008.2005605>
- [37] Serré, G., Boguslawski, E., Donnot, B., Pavao, A., Guyon, I., Marot, A.: Reinforcement learning for energies of the future and carbon neutrality: a challenge design (07 2022). <https://doi.org/10.48550/arXiv.2207.10330>
- [38] Silver, D., Hubert, T., Schrittwieser, J., Antonoglou, I., Lai, M., Guez, A., Lanctot, M., Sifre, L., Kumaran, D., Graepel, T., Lillicrap, T.P., Simonyan, K., Hassabis, D.: Mastering chess and shogi by self-play with a general reinforcement learning algorithm. *ArXiv abs/1712.01815* (2017), <https://api.semanticscholar.org/CorpusID:33081038>

- [39] Subramanian, M., Viebahn, J., Tindemans, S.H., Donnot, B., Marot, A.: Exploring grid topology reconfiguration using a simple deep reinforcement learning approach. In: 2021 IEEE Madrid PowerTech. IEEE (Jun 2021). <https://doi.org/10.1109/powertech46648.2021.9494879>
- [40] Taha, S., Poland, J., Knezovic, K., Shchetinin, D.: Learning to run a power network under varying grid topology. In: 2022 IEEE 7th International Energy Conference (ENERGYCON). pp. 1–6 (2022). <https://doi.org/10.1109/ENERGYCON53164.2022.9830198>
- [41] Viebahn, J., Kop, S., van Dijk, J., Budaya, H., Streefland, M., Barbieri, D., Champion, P., Jothy, M., Renault, V., Tindemans, S.: GridOptions tool: Real-world day-ahead congestion management using topological remedial actions (2024), <https://cse.cigre.org/cse-n035/c2-gridoptions-tool-real-world-day-ahead-congestion-management-using-topological-remedial-actions.html>, CIGRE Paris Session 2024
- [42] Viebahn, J., Naglic, M., Marot, A., Donnot, B., Tindemans, S.: Potential and challenges of AI-powered decision support for short-term system operations (2022), <https://research.tudelft.nl/en/publications/potential-and-challenges-of-ai-powered-decision-support-for-short>, cIGRE paris Session 2022 ; Conference date: 28-08-2022 Through 02-09-2022
- [43] Xu, P., Duan, J., Zhang, J., Pei, Y., Shi, D., Wang, Z., Dong, X., Sun, Y.: Active power correction strategies based on deep reinforcement learning—part i: A simulation-driven solution for robustness. CSEE Journal of Power and Energy Systems **8**(4), 1122–1133 (2022). <https://doi.org/10.17775/CSEEJPES.2020.07090>
- [44] Xu, P., Pei, Y., Zheng, X., Zhang, J.: A simulation-constraint graph reinforcement learning method for line flow control. In: 2020 IEEE 4th Conference on Energy Internet and Energy System Integration (EI2). pp. 319–324 (2020). <https://doi.org/10.1109/EI250167.2020.9347305>
- [45] Yoon, D., Hong, S., Lee, B.J., Kim, K.E.: Winning the L2RPN challenge: Power grid management via semi-markov afterstate actor-critic. In: International Conference on Learning Representations (2020), <https://openreview.net/forum?id=LmUJqB1Cz8>

- [46] Zhang, W., Sheng, Z., Jiang, Y., Xia, Y., Gao, J., Yang, Z., Cui, B.: Evaluating deep graph neural networks (2021), <https://arxiv.org/abs/2108.00955>
- [47] Zhao, Y., Liu, J., Liu, X., Yuan, K., Ren, K., Yang, M.: A graph-based deep reinforcement learning framework for autonomous power dispatch on power systems with changing topologies. In: 2022 IEEE Sustainable Power and Energy Conference (iSPEC). pp. 1–5 (2022). <https://doi.org/10.1109/iSPEC54162.2022.10033001>
- [48] Zhou, B., Zeng, H., Liu, Y., Li, K., Wang, F., Tian, H.: Action set based policy optimization for safe power grid management (2021). <https://doi.org/10.48550/arXiv.2106.15200>
- [49] Zhou, Y., Zamzam, A.S., Bernstein, A., Zhu, H.: Substation-level grid topology optimization using bus splitting. In: 2021 American Control Conference (ACC). pp. 1–7 (2021). <https://doi.org/10.23919/ACC50511.2021.9483070>